REDVET - Revista electrónica de Veterinaria - ISSN 1695-7504
Vol 25, No. 1S (2024)
http://www.veterinaria.org
Article Received- Revised- Accepted-

Insilico Analysis And Molecular Docking Studies Of Potential Compounds From Crateva Magna (Lour.) DC. Using POAP

Shinsy Poongattil [1], Jibu Thomas[2*], Christy Joy[3]

[1,3]Department of Biotechnology, Karunya Institute of Technology and Sciences, Karunya Nagar, Coimbatore
[2*]Professor and Head , Department of Biotechnology, Karunya Institute of Technology and Sciences, Coimbatore, Tamil Nadu, India. Email: jibuthomas@karunya.edu

Abstract
In silico analysis provides an accelerated screening method to identify potential bioactive compounds in plant extracts. Though *Crateva magna's* application in traditional medicine is well documented, the bioactivity of its secondary metabolites are not extensive. Gas Chromatography-Mass Spectroscopy (GC-MS) analysis of methanolic extracts of root, bark, flower and leaves of *Crateva magna* revealed numerous compounds. Virtual screening was performed using POAP against 57 proteins encompassing antimicrobial targets and those implicated in human diseases. Evaluation of docked complexes with scores above -9.6 revealed ligands interacts strongly with 10 protein targets. Leaf extract based compound, Butane, 1,4-bis(9,10-dihydro-9-methylanthracen-10-yl)-, a reported bioherbicide showed strong affinity to multiple targets of *Staphylococcus aureus*, SARS Cov2 and opportunistic *Candida albicans.* Isoquinoline, 1-[(3,5-dibenzyloxy)benzyl]-1,2,3,4- tetrahydro-6-methoxy- interacted strongly with diabetic protein targets in addition to antimicrobial proteins. The multitude of novel bioactive compounds detected in *Crateva magna* by GC-MS followed by virtual screening would pave the way for identifying potential drug candidates.

Keywords: POAP, Binding affinity, GNU parallel pipeline, Drug design, Binding pocket prediction, *Crateva magna* (Lour.)DC.

Abbreviations

GC-MS	Gas Chromatography-Mass spectrometry
HPTLC	High-performance thin-layer chromatography
POAP	Parallelized Open Babel and Auto Dock Suite Pipeline
GNU	GNU's Not Unix
ADMET	Chemical adsorption, distribution, metabolism, excretion and toxicity

1.INTRODUCTION

Crateva magna (Lour.) DC., is a medium sized deciduous tree belonging to the family Capparidaceae and commonly called a three-leaved caper, predominantly found in the semiarid regions of the Indian subcontinent. Anti-inflammatory, antihypertensive, antihyperglycemic, and analgesic activity has been reported in this plant (Premila, 1995). It is frequently preferred in the treatment of urinary disorders in Ayurveda and Unani medicine since it promotes removal of kidney stones (Bopana & Saxena, 2008). Lupeol, a pentacyclic triterpene isolated from the root bark of *C magna* significantly curtailed the deposition of stone-formation in kidneys(Sethi et al., 1978). The high phenolic content in the aqueous extracts of stem, bark, and leaves showed significant capacity to inhibit the activity of α-glucosidase and α-amylase, and thus makes the plant species a potential, nutraceutical source in the management of diabetes (Loganayaki & Manian, 2012). The administration of *C. magna* extract significantly reduced the elevated glucose levels in alloxan-induced diabetic rats, confirming its anti-diabetic activity (Prabhat et al., 2010).

While a vast array of bioactive molecules are known to be present across plant species, the identification of these compounds remains one of the limiting factors. Spectrometric and chromatographic methods are ideal techniques to rapidly screen and identify the chemical composition and pharmacological effects of bioactive compounds present in plant species (Juszczak et al., 2019). High-performance thin-layer chromatography (HPTLC) of *Crateva magna* extracts collected from various south Indian locations revealed the presence of distinctive bands upon comparison, highlighting metabolites variability in the same species collected from different environment (Poongattil et al., 2024). Gas Chromatography-Mass spectrometry (GC-MS) is one of the widely employed techniques for the identification of various bioactive compounds present in medicinal plants, aided by the requirement of small sample volume and accuracy (Fan et al., 2018). Bioactivity evaluation of natural compounds identified in plant extracts through *in vitro*

analysis is costly and time consuming. *In silico* analysis provides a rapid and cost-effective alternative to *in vitro* biological assays (Shaker et al., 2021).

Virtual screening is a technique used to discover novel ligands for protein structure and plays an important role in structure-based drug design. Molecular docking provides information about drug-receptor interactions, facilitating predictions regarding the binding orientation of drug candidates to their target proteins (Lee & Kim, 2019). Recently compounds identified by GC-MS analysis of *Multidentia crassa* were evaluated for their anti-inflammatory and analgesic activity using virtual screening (Chikowe et al., 2024). Though active compounds from the root extract of *C. magna* have been reported (Vijayakumari et al., 2016), their potential bioactivity identified through virtual screening has not been widely reported. Hence this study aims to identify bioactive molecules targeting various human metabolic disorders as well as pathogenic microorganisms. The methanolic extracts of bark, flower, leaf, and root of *C. magna* were subjected to GC-MS analysis. Compounds identified in the extracts were then screened for their potential interaction with target proteins using molecular docking.

2.Materials & Methods

2.1. Preparation and extraction of plant materials

Plant specimens of *C. magna* were collected from Coimbatore, Tamil Nadu. The roots and aerial parts including flowers, leaves, and bark were rinsed with distilled water and air-dried for a week in the shade. The plant materials were then pulverised using a food-grade grinder separately and preserved in airtight containers at room temperature. For extraction, 5 g of each sample (powdered root, flower, leaves, and bark) was subjected to reflux extraction using methanol as solvent. The extracts were filtered through Whatman filter paper Grade 1 to remove the powder residues. Each solvent mixture was concentrated using a rotary evaporator and used for GC–MS analysis.

2.2. Gas Chromatography-Mass Spectrometry Analysis (GC-MS)

Identification of compounds was performed using GC-MS. The analysis of different methanol extracts was performed using a Thermo Scientific, Single Quadrupole MS, TG-5MS fused silica capillary column (30 m, 0.251 mm, 0.1 mm film thickness). For detection, an electron ionization system with an ionization energy of 70 eV was used. Helium was used as the carrier gas at a constant flow rate of 1 mL/min. 1 µL volume of sample is injected for the analysis. The injector and MS transfer line temperature was set at 280 °C. The initial temperature of the oven was programmed at 40 °C (hold for 3 min) with the final temperature of 280 °C at an increasing rate of 5 °C/min (hold 5 min). Identification of the compounds was performed based on the comparison of their relative retention time and mass spectra with those of the NIST library data of the GC-MS system (Hebbar & Nalini, 2020). The NIST library probability score is a measure of similarity between a compound in the sample given in a peak in a GC-MS analysis and known compounds catalogued in the NIST library (Oberacher et al., 2013).

2.3. Ligand Preparation

The Pubchem database was used to obtain the 3D structural data files (sdf) of the ligands found in the GC-MS analysis of various C. magna methanol extracts. The Parallelized Open Babel and Auto Dock Suite Pipeline (POAP), which is a GNU parallel based pipeline, (Samdani & Vetrivel, 2018) ligand preparation module, which incorporates the Open Babel tool, was utilised to prepare the ligands. A weighted rotor approach was used to create 50 conformers for each ligand after creating 3D coordinates. From here, the conjugate gradient approach with 5000 steps was used to minimise energy in the ligand conformer with the lowest energy. These ligands with reduced energy were utilised for virtual screening after being converted to pdbqt format.

2.4. Target protein preparation

3D conformations of 57 proteins implicated in various diseases were retrieved from PDB database. Each protein structures were then analyzed and their reduntant hetero groups and homologous chains were eliminated. The structures were then fine-tuned by the addition of Kollman charges and polar hydrogen atoms using Autodock (Morris et al., 2009). Following energy minimization, the pdbqt files were generated for all the protein targets, and identification of their binding sites was performed using Discovery Studio Visualizer (Bovia, 2019).

2.5. Virtual screening

The POAP multiple receptor virtual screening module of AutoDock Vina was used to virtually screen the targets (Trott & Olson, 2009). Using the MGLTOOLS-1.5.6, the receptors were constructed by adding gastieger charges and polar hydrogens. Docking was carried out with an exhaustiveness of eight using an input file that contained the configuration for each target protein's active site. Protein-ligand complex architectures and docking scores were categorised into several folders. The best ligands and their receptor targets were filtered out using a strict docking score of -9.6 or above. The amino acid 2D interaction diagrams were obtained using Biovia DSV(Joy & Cyriac, 2022).

REDVET - Revista electrónica de Veterinaria - ISSN 1695-7504
Vol 25, No. 1S (2024)
http://www.veterinaria.org
Article Received- Revised- Accepted-

3.Results

3.1.Identification of compounds in *C.magna* extracts using GC-MS

The GC-MS analysis of methanolic extracts of different parts (Flower, leaf, bark, and root) of *C. magna* identified numerous compounds which are listed in the Table (Supplementary S1)

3.2. Virtual screening

The compounds (ligands) identified by GC-MS analysis were further screened for potential pharmacological activity through *in silico* analysis. The proteins which are implicated in diabetes, cardiovascular, hepatic, neuronal diseases, and known drug targets of viral, fungal, and bacterial pathogens were used as targets for virtual screening with the ligands. List of proteins with their PDB IDs is summarised in (Supplementary table S2). Docked complexes which have docking scores of more than -9.6 were then analysed for their interactions.

3.3. Antifungal study using docking

One of the opportunistic fungus, *Candida albicans* is known to reside within various anatomical regions of the human body. It causes severe health issues, mainly targeting the oral, reproductive, and gastro-intestinal regions especially when the immune system is weak (Jabra-Rizk et al., 2016). Thus finding potential drugs against *Candida albicans* is paramount. We analysed three major targets against *Candida albicans* namely the N-myristoyltransferase, dihydrofolate reductase, and secreted aspartyl proteinases. N-myristoyltransferase plays a key role in post-translational modifications of proteins, thus aiding in proliferation and pathogenesis of *Candida sps.* (Weinberg et al., 1995). Dihydrofolate reductase (DHFR), a known antifungal target, is a regulatory component of the nucleic acid synthesis(Paulsen et al., 2011). Secreted aspartyl proteinases, a major virulence protein, is involved in digestion of host membrane as well as negatively modulates immune response thus enhances *Candidas sps.* pathogenicity (Staniszewska et al., 2012).

Our virtual screening identified that 9-Phenanthrenemethyl 2,6- Dimethylbenzoate, and Butane, 1,4-bis (9,10-dihydro-9- methylanthracen-10-yl)-, binds with high affinity to *Candida albicans* dihydrofolate reductase (4HOF) with a docking score of -9.8 (Table 1, Figure 1) highlighting the potential application of these compounds as selective antifungal inhibitors. No potential binding partners were detected for the other two antifungal targets, N-myristoyltransferase and secreted aspartyl proteinases.

Table 1: Binding score and interacting residues of top ligands to fungal drug targets

PDB ID	Protein	Pubchem ID	Ligand	Docking score	Extract	Interacting residue
4HOF	DHFR *(Candida Albicans)*	605632	9-Phenanthrenemethyl 2,6-dimethylbenzoate	-9.8	Leaf	Ala 11,Met 25,Phe 26, Ile 32, Lys 37, Leu 69, Ile 112
		606355	Butane, 1,4-bis(9,10-dihydro-9-methylanthracen-10-yl)-	-9.8	Leaf	Met 25, Phe 36, Ile 33, Lys 37,Ile 62, Pro 63, Phe 66, Leu 69, Pro 70

REDVET - Revista electrónica de Veterinaria - ISSN 1695-7504
Vol 25, No. 1S (2024)
http://www.veterinaria.org
Article Received- Revised- Accepted-

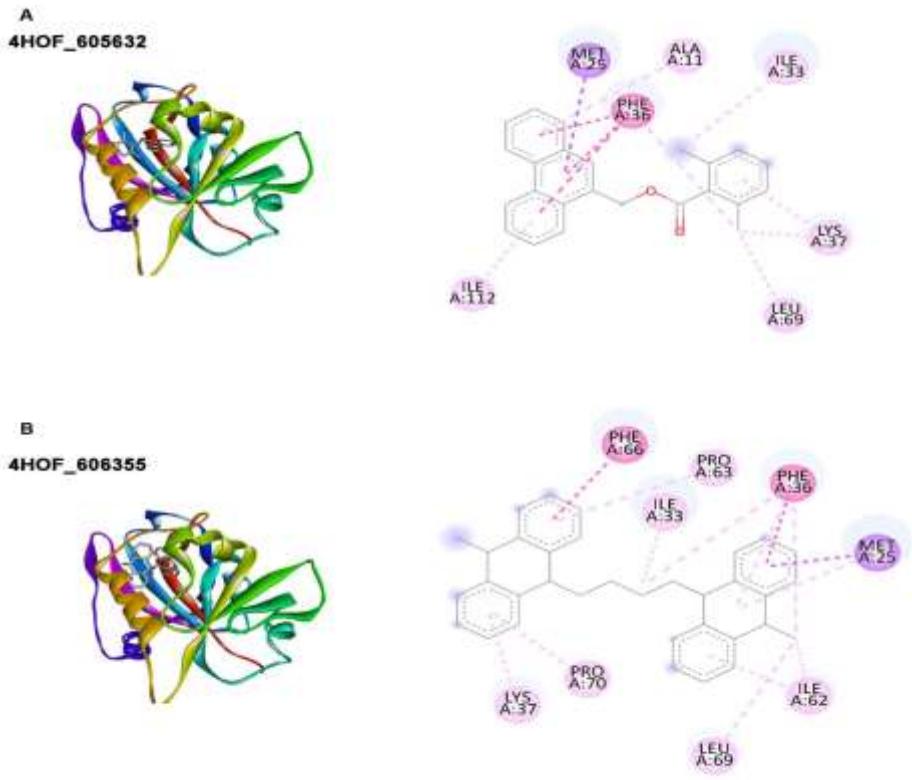

Figure 1: Docked complex of ligands with DHFR of candida albicans

A)DHFR with 9-Phenanthrenemethyl 2,6-Dimethylbenzoate; B) DHFR with Butane, 1,4-bis(9,10-dihydro-9-methylanthracen-10-yl)-

3.4. Antiviral study using docking

The pandemic and frequent epidemics caused by various viruses, have revealed the lacuna in the pharmaceutical industry in identifying antiviral drugs. M (pro), a SARS-COV2 protease is involved in the replication and maturation of the viral particle, is an optimal target for drug intervention. The Histidine(41)-Cysteine (145) catalytic dyad of the protease serves as a pivotal binding site for designing of drug molecules (Jin et al., 2020; Lu et al., 2006). Another probable target against SARS-COV2 is the macro domain region of nonstructural protein 3 (NSP3). Its diverse roles include abrogating the immune responses while aiding in its replication (Jin et al., 2020).

The virtual screening showed that Butane, 1,4-bis(9,10-dihydro-9-methylanthracen-10-yl)- and 2H-1-Benzopyran, 2,2-diphenyl-, identified in the leaf extract showed significant binding to the macro domain region of NSP3 with a docking score of -9.7 and -9.6 respectively (Table 2, Figure 2). Interestingly, Butane, 1,4-bis(9,10-dihydro-9-methylanthracen-10-yl)- also showed interaction with M (pro) with a docking score of -9.8. These interactions emphasise the compound's capacity to act as a negative regulator of SARS COV-2 viral proliferation by acting on multiple targets. Similarly, Isoquinoline, 1-[(3,5-dibenzyloxy)benzyl]-1,2,3,4- identified in the root extract also showed interaction with M (pro) protein with a docking score of -9.6 (Table 2, Figure 2).

Table 2: Binding score and interacting residues of top ligands to viral drug targets

PDB ID	Protein	Pubchem ID	Ligand	Docking score	Extract	Interacting residue
7CZ4	NSP3 (macro domain)	271528	2H-1-Benzopyran, 2,2-diphenyl-	-9.6	Leaf	Ser 80
		606355	Butane, 1,4-bis(9,10-dihydro-9-methylanthracen-10-yl)-	-9.7	Leaf	Lys 76, Val 82, Leu 93

2GZ9	M Pro	606355	Butane, 1,4-bis(9,10-dihydro-9-methylanthracen-10-yl)-	-9.8	Leaf	Ile 249, Pro 293, Leu 202, Phe 294
		595533	Isoquinoline, 1-[(3,5-dibenzyloxy)benzyl]-1,2,3,4-tetrahydro-6-methoxy-	-9.6	root	Asp 153,Leu 202, Pro 293, Phe 294, Asp 295, Val 297,

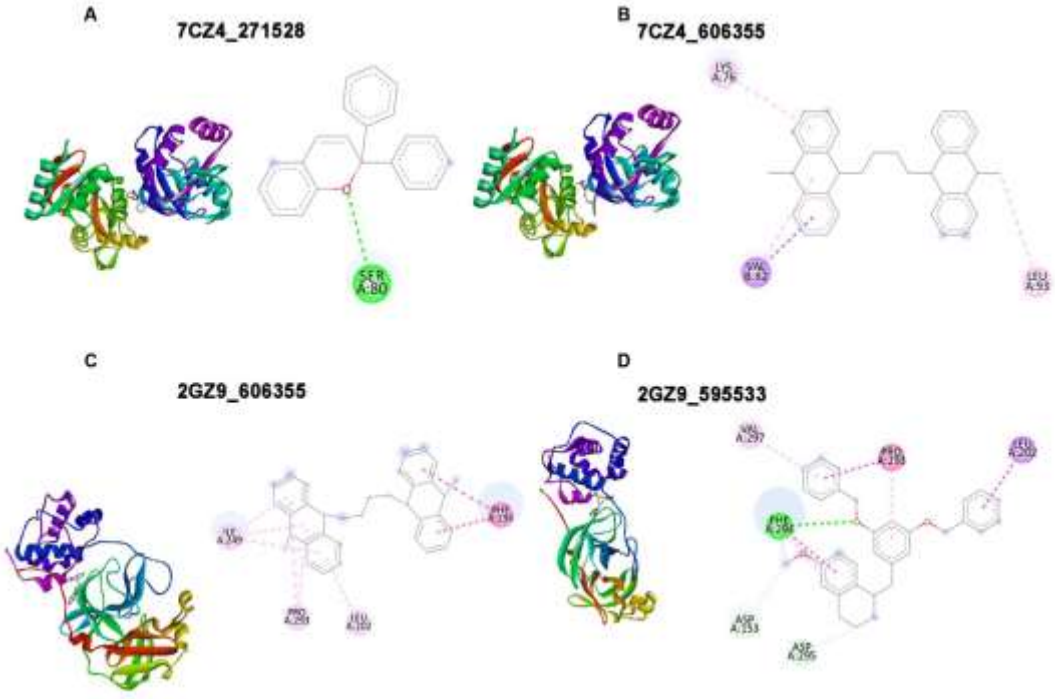

Figure 1: Docked complex of ligands with target proteins of SARS CoV2

A)NSP3 with 2H-1-Benzopyran, 2,2-diphenyl-; B)NSP3 with Butane, 1,4-bis(9,10-dihydro-9-methylanthracen-10-yl)-; C) M Pro with Butane, 1,4-bis(9,10-dihydro-9-methylanthracen-10-yl)-; D)M Pro with Isoquinoline, 1-[(3,5-dibenzyloxy)benzyl]-1,2,3,4- tetrahydro-6-methoxy-

3.5. Antibacterial study using docking

With an increase in multidrug resistant bacterial infections, identifying potential drug candidates is important. *Staphylococcus aureus,* an opportunistic bacteria, has gained notoriety due to its multi drug resistance especially against methicillin based antibiotics. Dihydrofolate reductase (DHFR), a key enzyme in the folate synthesis, is a potential antibacterial target (Bourne et al., 2010; Singh et al., 2022). DNA Gyrase B which aids in replication by inducing negative supercoiling in DNA has been proposed as a potential target to overcome the antibiotic resistance in *Staphylococcus aureus* (Durdagi et al., 2018). Rhomboid protease Glp of *E. coli* is essential for extraintestinal pathogenic *E. coli* to localise within the mucus regions and supports its survival. The pathogenic *E. coli* strains are known to cause urinary tract infections and sepsis in neonates which can lead to mortality (Russell et al., 2017).

The virtual screening revealed that Butane, 1,4-bis(9,10-dihydro-9-methylanthracen-10-yl)-, Dibenzo(a,c)fluoren-13-one, and 7H-Dibenzo(a,g)carbazole, 12,13- dihydro- identified in the leaf extract was shown to interact with *S. aureus* DHFR and Gyrase B (Table 3;Figure 3,4), suggesting its antibacterial potential by effectively targeting multiple proteins. In addition, 3-Pyrrol5-[2-(1H-benzoimidazol-2-yl)-2-cyanovinyl]furan-2-yl morphobenzoic acid in the bark extract also binds to *S. aureus* Gyrase B (Table 3; Figure 4). Pyrimidine-2,4,6(1H,3H,5H)-trione, 5- [3-[2-(4-tertbutylphenoxy)ethoxy]benzylidene]-of root extract, 3-Pyrrol 5-[2-(1H-benzoimidazol-2-yl)-2-cyanovinyl]furan-2-ylmorphobenzoic acid of bark extract and D-Bicuculline identified in flower extract showed interactions with DHFR of *S. aureus* (Figure 3). The structures of other ligands docked with DHFR of *S. aureus* are in Supplementary (Figure S2). The Glp protease of *E. coli* was observed to bind with nine different ligands identified in the GCMS of leaf, bark and root extract. Among them, the highest docking score of -11.0 was observed for the ligand 7H-Dibenzo(a,g)carbazole, 12,13- dihydro- (leaf extract) followed by Pyrimidine-2,4,6(1H,3H,5H)-trione,5-[3-[2-(4-

tertbutylphenoxy)ethoxy]benzylidene]- of root extract with a score of -10.4 (Table 3; Figure 4). The structures of other ligands docked with Glp protease shown in Supplementary (Figure S3).

Table 3: Binding score and interacting residues of top ligands to bacterial drug targets

PDB ID	Protein	Pubchem ID	Ligand	Docking score	Extract	Interacting residue
3FYV	DHFR (S. aureus)	10237	D-Bicuculline	-9.9	Flower	Leu 20, Val 31, Phe 92, Leu 28, Gly 15, Thr 121, Ile 14, Asn 18, Ser 49, Ala 7
		181908	di[1-(3,4-methylenedioxyphenyl)-2-propyl]methylamine	-9.6	Bark	
		5286533	3-Pyrrol5-[2-(1H-benzoimidazol-2-yl)-2-cyanovinyl]furan-2-ylmorphobenzoic acid	-10.4	Bark	
		5379632	Pyrimidine-4,6-dione, hexahydro-5-[3-[2-(4-methylphenoxy)ethoxy]benzylidene]-2-thioxo-	-9.7	Bark	
		91730889	4-Fluoro-2-trifluoromethylbenzoic acid, 2,4-dichloronaphthyl-1 ester	-9.8	Bark	
		580552	Lycorenan-7-one, 5-hydroxy-1-methyl-9,10-[methylenebis(oxy)]-, (5.alpha.)-	-9.9	Root	Thr 46, Ile 14, Ala 7, Phe 92, Val 6, Leu 20, Val 31
		633813	Pyrimidine-2,4,6(1H,3H,5H)-trione, 5-[3-[2-(4-tertbutylphenoxy) ethoxy]benzylidene]-	-10	Root	Gly 94, Lys 45, Phe 92, Ala 7
		595533	Isoquinoline, 1-[(3,5-dibenzyloxy)benzyl]-1,2,3,4-tetrahydro-6-methoxy-	-9.8	Root	Phe 92, Leu 28, Ala 7, Val 31, Leu 20, Asn 18, Thr 121, Lys 45, Gln 95
		627194	Pyrimido[1,2-a]indole, 4-isopropyl-5-methyl-2-phenyl-	-9.5	Root	Phe 92, Val 32,Val 6, Leu 20, Leu 28
		44387	7H-Dibenzo(a,g)carbazole, 12,13-dihydro-	-10.6	Leaf	Ile 14, Lue 20, Ala 7, Phe 92
		187380	Dibenzo(a,c)fluoren-13-one	-10.6	Leaf	Leu 28, Val 31, Leu 20, The 46, Ala 7, Ile 14
		605632	phenanthren-9-ylmethyl 2,6-dimethylbenzoate	-9.9	Leaf	Lys 45, The 121, Ile 14, Leu 20
		606355	Butane, 1,4-bis(9,10-dihydro-9-methylanthracen-10-yl)-	-11.3	Leaf	Leu 20, Val 31, Leu 20, Thr 46, Ile 14, Ala 7
		624636	7H-Dibenzo[b,g]carbazole, 7-methyl-	-10.5	Leaf	Val 6, Ala 7, Phe 98, Val 31, Leu 20, Ile 14
3ZMI	Rhomboid protease GlpG *(E. coli)*	96896	Benzo(b)phenazine	-9.8	Bark	
		268932	Benzo(b)naphtho(1,2-d)furan	-9.8	Bark	

3ZMI	Rhomboid protease GlpG *(E. coli)*	91727615	Diglycolic acid, di(pentafluorobenzyl) ester	-9.8	Bark	
		91730889	4-Fluoro-2-trifluoromethylbenzoic acid, 2,4-dichloronaphthyl-1 ester	-9.6	Bark	
		70385	2H-1-Benzopyran-2-one, 3-phenyl-	-9.7	Root	Met 149, Trp 236, Trp 157, Tyr 205, Val 204,Met 208, Ser 201, His 150
		633813	Pyrimidine-2,4,6(1H,3H,5H)-trione, 5-[3-[2-(4-tertbutylphenoxy) ethoxy]benzylidene]-	-10.4	Root	Met 208, Val 204, Ser 201, His 150, Gly 198, Tyr 205, His 254, Ala 250
		939955	6-Trifluoromethyl-benzo[4,5]imidazo[1,2-c]quinazoline	-9.7	Root	Val 204, Met 208, Trp 157, Tyr 205, His 254, Gly 240, Trp 236
		44387	7H-Dibenzo(a,g)carbazole, 12,13-dihydro-	-11	Leaf	Val 204, Met 208, Tyr 205, Trp 157, Trp 236, Met 149
		624636	7H-Dibenzo[b,g]carbazole, 7-methyl-	-10	Leaf	Trp 157, Val 204, Met 208, Tyr 205, His 254, Met 149, Trp 236
4URM	DNA GyraseB *(S. aureus*)	5286533	3-Pyrrol5-[2-(1H-benzoimidazol-2-yl)-2-cyanovinyl] furan-2-ylmorphobenzoic acid	-9.8	Bark	Ile 175, Ile 86, Asn 54, Asp 57, Ala 61, Asp 81, Ser 55
		44387	7H-Dibenzo(a,g)carbazole, 12,13-dihydro-	-9.6	Leaf	Val 204, Trp 157, Met 208, Tyr 205, Trp 236, Met 149
		187380	Dibenzo(a,c)fluoren-13-one	-9.7	Leaf	Ile 51, Ile 175, Ser 128, Ile 86, The 173, Gly 85, Ile 102
		606355	Butane, 1,4-bis(9,10-dihydro-9-methylanthracen-10-yl)-	-10.1	Leaf	Asn 54, Ile 86, Ile 102, Pro 87, Arg 84, Ala 61, Glu 58

REDVET - Revista electrónica de Veterinaria - ISSN 1695-7504
Vol 25, No. 1S (2024)
http://www.veterinaria.org
Article Received- Revised- Accepted-

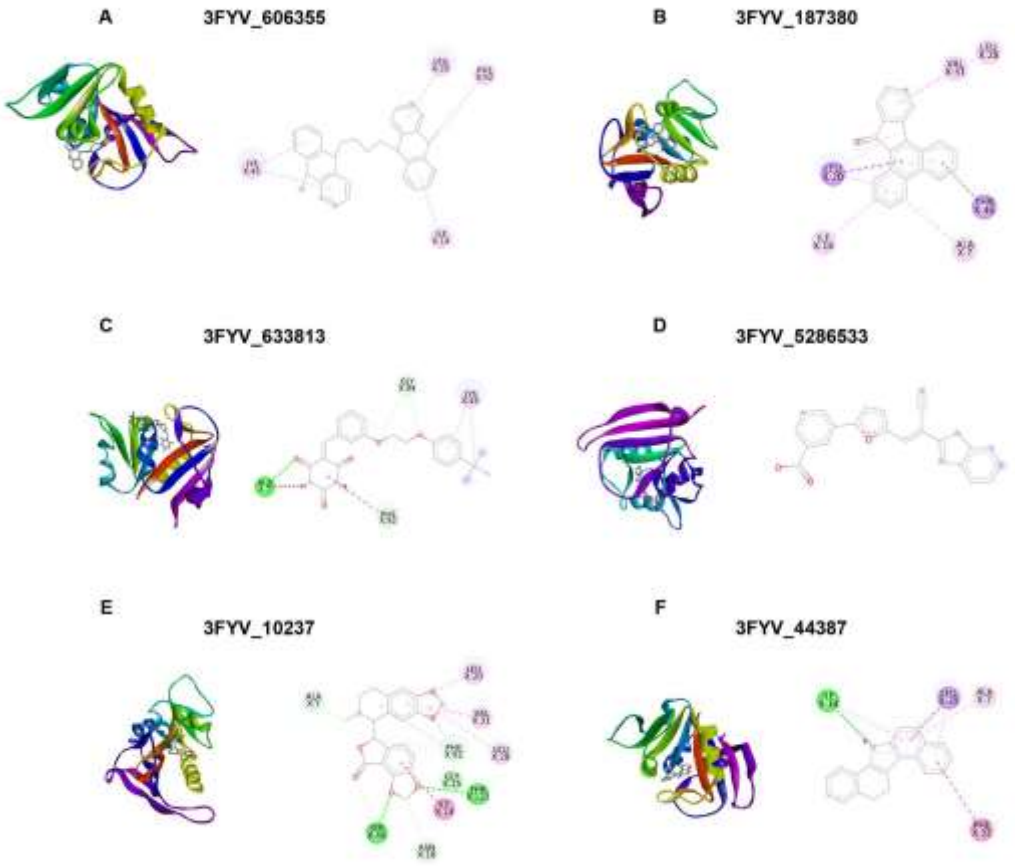

Figure 3: Docked complex of ligands with DHFR of *S. aureus*

A) Butane, 1,4-bis(9,10-dihydro-9-methylanthracen- 10-yl)- ;B) Dibenzo(a,c)fluoren-13-one;
C) Pyrimidine-2,4,6(1H,3H,5H)-trione, 5- [3-[2-(4-tertbutylphenoxy) ethoxy]benzylidene]-;
D)3-Pyrrol5-[2-(1H-benzoimidazol-2-yl)-2-cyanovinyl]furan-2-ylmorphobenzoic acid; E) D-Bicuculline;
F) 7H-Dibenzo(a,g)carbazole, 12,13-dihydro-

REDVET - Revista electrónica de Veterinaria - ISSN 1695-7504
Vol 25, No. 1S (2024)
http://www.veterinaria.org
Article Received- Revised- Accepted-

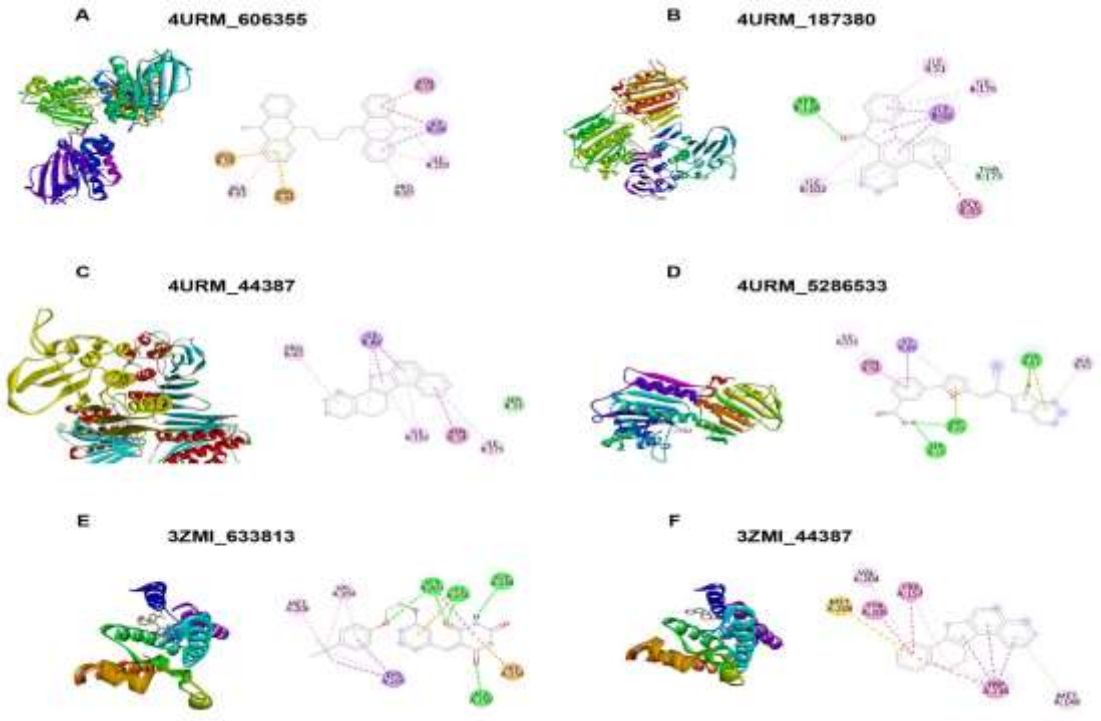

Figure 4: Docked complex of ligands with DNA Gyrase B of *S. aureus* and Rhomboid protease Glp of *E. coli.*

A) DNA gyrase with Butane, 1,4-bis(9,10-dihydro-9-methylanthracen- 10-yl)-; B) DNA gyrase with Dibenzo(a,c)fluoren-13-one; C) DNA gyrase with 7H-Dibenzo(a,g)carbazole, 12,13-dihydro-; D) DNA gyrase with 3-Pyrrol5-[2-(1H-benzoimidazol-2-yl)-2-cyanovinyl]furan-2-ylmorphobenzoic acid; E)Glp protease with Pyrimidine-2,4,6(1H,3H,5H)-trione, 5-[3-[2-(4-tertbutylphenoxy) ethoxy]benzylidene]-; F) Glp protease with 7H-Dibenzo(a,g)carbazole, 12,13- dihydro-.

3.6. Inhibitors for metabolic, neurological disorders and cancer

A total of 29 proteins identified as chief targets for cardiovascular, respiratory, hepatic, metabolic and neurological disorders in humans were used for molecular docking. Out of these, four protein targets showed interactions with multiple ligands with a docking score of -9.6 or higher. Pyruvate dehydrogenase complex (PDC) modulations are known to play a key role in progression of diseases like diabetes, ischemia and cancer. The activity of PDC is controlled by the pyruvate dehydrogenase kinase (PDK) family (Jeoung, 2015; Wang et al., 2021). Loss of PDK 2 has shown significant reduction in blood glucose levels (Jeoung et al., 2012). It is also implicated in progression of various kinds of cancer (Michelakis et al., 2010; Sameen et al., 2011; Sun et al., 2017). 2H-1-Benzopyran-2-one, identified in root extract, showed binding with PDK 2 (PDB ID: 4mp2) with a docking score of -9.6 (Table 4). Since PDK 2's role in multiple disorders is well established, the compound could have potential application in treatment of these disorders.

Dopamine, a major neutrotransmitor's dysregulation manifests in major neurological disorders like Parkinson's, Schizophrenia (Birtwistle & Baldwin, 1998) . Dopamine exerts its effect by binding to specific dopamine receptors. The dopamine receptor 2 is a known target for anti-phsychotic drugs (Li et al., 2016). 3-Pyrrol5-[2-(1H-benzoimidazol-2-yl)-2-cyanovinyl]furan-2-ylmorphobenzoic acid identified in the bark extract and Isoquinoline, 1-[(3,5-dibenzyloxy)benzyl]-1,2,3,4- tetrahydro-6-methoxy- present in the root extract interacted with Dopamine receptor D2 with the docking scores of -10.1, and -10.0 respectively(Figure 5, Table 4).

Type 2 diabetes manifests in the form of increased blood glucose levels due to insulin resistance. A recent molecule suggested to combat the issue of diabetes is Glucokinase, which is involved in glucose homeostasis. Increasing the activity of glucokinase could potentially alleviate diabetes (Ren et al., 2022; Sharma et al., 2022). 14 compounds of different extracts of *C. magna* showed binding to the glucokinase with a docking score ranging from -11.8 to -10.2. 7H-Dibenzo(a,g)carbazole, 12,13- of the leaf extract showed the best interaction (Table 5; Figure S4).

A recent study has highlighted the importance of the hydrophobic interaction of Tyrosine 214 and Valine 455 of glucokinase with the ligand 2-amino-4-fluoro-5-[(1-methyl-1h-imidazol-2-yl)sulfanyl]-n-(1,3-thiazol-2-yl)benzamide) (Ren et al., 2022). In our study, these interactions are also present, highlighting that these compounds could also act as activators of glucokinase, and considered potential anti-diabetic agents. Isoquinoline, 1-[(3,5-dibenzyloxy)benzyl]-

REDVET - Revista electrónica de Veterinaria - ISSN 1695-7504
Vol 25, No. 1S (2024)
http://www.veterinaria.org
Article Received- Revised- Accepted-

1,2,3,4- tetrahydro-6-methoxy- of root extract showed high affinity for glucokinase with a docking score -11.6(Figure 5, Table 5).

11β-Hydroxysteroid Dehydrogenases(11β-HSD), is a key enzyme in the cortisol synthesis (Chapman et al., 2013). 11β-HSD1 induces diabetes through insulin resistance (Peng et al., 2016). 13 compounds from all the 4 extracts of *C. magna* showed interactions with 11β-HSD (PDB ID:4K1L) (Table 4, Figure S5). Among them Butane, 1,4-bis(9,10-dihydro-9-methylanthracen- 10-yl)- of leaf extract showed affinity with a score of -11.2. Interestingly, isoquinoline, 1-[(3,5-dibenzyloxy)benzyl]-1,2,3,4- tetrahydro-6-methoxy- of root extract shown to have high affinity for glucokinase also showed affinity to 11β-HSD with a score of -11.0 (Figure 5). This highlights the molecule's capacity to potentially treat diabetes by modulating multiple targets.

Table 4: Binding score and interacting residues of top ligands to human disease protein targets

PDB ID	Protein	Pubchemi ID	Ligand	Docking score	Extract	Interacting residue
4IXC	Human Glucokinase activator	44387	7H-Dibenzo(a,g)carbazole, 12,13-dihydro-	-11.8	Leaf	Trp 99, Val 455, Gly 68, Tyr 214, Leu 451, Ile 211
		271528	2H-1-Benzopyran, 2,2-diphenyl-	-11.7	Leaf	Met 235, Met 210, Tyr 214, Ile 211, Val 455, Val 452, Val 62
		595533	Isoquinoline, 1-[(3,5-dibenzyloxy)benzyl]-1,2,3,4-tetrahydro-6-methoxy-	-11.6	Root	Tyr 215, Arg 63, Ile 159, Val 62, Ala 456, Val 455, Lys 459, Met 235, Tyr 214, Ile 211, Leu 451, Trp 99
		605632	phenanthren-9-ylmethyl 2,6-dimethylbenzoate	-11	Leaf	Leu 451, Val 455, Ile 211, Met 210, Gly 68, Tyr 214, Met 235
		91732132	2-(Perfluorobenzamido)ethyl 2,3,4,5,6-pentafluorobenzoate\	-10.8	Leaf	Tyr 215, Thr 65, Ser 64, Cys 220, Glu 221, Tyr 214, Met 210, Met 235, Ile 211, Leu 451, Ser 69
		139972	1,3,3-Triphenylazetidin-2,4-dione	-10.7	Flower	Val 62, Glu 67, Gly 68,Ser 69, ILE 211, Tyr 214, Val 452, Val 455
		410836	2,2-Bis-(4-dimethylamino-phenyl)-1-phenylethanone	-10.6	Leaf	Arg 63, Tyr 61, Val 452, Ala 456, Leu 451, Val 62, Val 455, Ile 211, Tyr 215, Tyr 214, Met 210, Met 235
		633813	Pyrimidine-2,4,6(1H,3H,5H)-trione, 5-[3-[2-(4-tertbutylphenoxy) ethoxy]benzylidene]-	-10.6	Root	Val 455, Ile 211, Arg 63, Lys 459, Ile 159, Ala 456, Ser 64, Met 235, Thr 65, Tyr 214

		268932	Benzo(b)naphtho(1,2-d)furan	-10.4	Bark	
		5379632	Pyrimidine-4,6-dione, hexahydro-5-[3-[2-(4-methylphenoxy)ethoxy]benzylidene]-2-thioxo-	-10.4	Bark	
		91730889	Pyrimidine-4,6-dione, hexahydro-5-[3-[2-(4-methylphenoxy)ethoxy]benzylidene]-2-thioxo-	-10.4	Bark	Ser 69, Leu 451, Met 210, Ser 64, Tyr 214, Ile 211, His 218, Tyr 215, Glu 67
		181908	di[1-(3,4-methylenedioxyphenyl)-2-propyl]methylamine	-10.3	Bark	Ser 69, Trp 99, Val 62, Met 210, Met 235, Ile 211, Tyr 214, Leu 451, Tyr 215
		69779	Diphenyl isophthalate	-10.2	Root	Trp 99, Tyr 215, Leu 451, Ile 211, Val 455, Met 235, Tyr 214
4IXC	Human Glucokinase	296571	Cyclohexane, 1,1'-[4-(3-cyclohexylpropyl)-1,7-heptanediyl]bis-	-10.2	Root	Val 62, Arg 63, Trp 99, Ile 211,Tyr 214, Tyr 215,Met 235,Leu 451, Val 452, Val 455
4K1L	11 beta-HSD1	606355	Butane, 1,4-bis(9,10-dihydro-9-methylanthracen-10-yl)-	-11.2	Leaf	Val 180, Tyr 177, Leu 126, Ala 172, Ala 223, Ile 218, Leu 215, Val 168, Ile 46, Ile 121, Leu 217, Tyr 183
		595533	Isoquinoline, 1-[(3,5-dibenzyloxy)benzyl]-1,2,3,4-tetrahydro-6-methoxy-	-11	Root	Ala 226, Leu 217, Val 180, Tyr 177, Ala 172, Ala 223, Gly 216, Ile 121, Ile 46, Lys 44, Gly 41, Asn 119
		605632	phenanthren-9-ylmethyl 2,6-dimethylbenzoate	-10.8	Leaf	Tyr 183, Val 227, Val 180, Leu 171, Tyr 177, Ala 172, Leu 217, Ala 223
		173183	Campesterol	-10.6	Bark	
		619612	2-Methyl-2H-pyrazole-3-carboxylic acid [2-(5-benzyloxy-2-methyl-1H-indol-3-yl)-ethyl]-amide	-10.5	Leaf	Lys 44, Arg 66, Gly 91, Thr 92, Met 93, Ile 121, Val 142, Leu 215

		92157	Urs-12-en-3-ol, acetate, (3.beta.)-	-10.5	Root	Ile 46, Ile 121, Leu 217, Ala 223, Tyr 183
		44387	7H-Dibenzo(a,g)carbazole, 12,13-dihydro-	-10.4	Leaf	Asn 119, Ile 121, Val 168, Leu 215, Ile 218
		5286533	3-Pyrrol5-[2-(1H-benzoimidazol-2-yl)-2-cyanovinyl] furan-2-ylmorphobenzoic acid	-10.2	Bark	Ile 121, Ile 218, Ala 223, Ile 46, Gly 47, Gly 41, Ala 65
		633813	Pyrimidine-2,4,6(1H,3H,5H)-trione, 5-[3-[2-(4-tertbutylphenoxy) ethoxy]benzylidene]-	-10.2	Root	Ala 65, Ile 121, Ile 46, Lys 44, Val 142, Asn 123, Arg 66, Met 93
		187380	Dibenzo(a,c)fluoren-13-one	-10.1	Leaf	Ala 172, Val 180, Tyr 177, Thr 222, Ala 226, Ala 223
		630919	4-Phenoxy-5,6-diphenyl-2H-pyridazin-3-one	-10.1	Root	Ala 226, Ile 218, Ala 223, Tyr 183, Leu 215, Leu 171, Ala 172, Val 180, Leu 126, Tyr 177
		10237	D-Bicuculline	-9.9	Flower	Ala 223, Thr 124, Ala 226, Leu 215, Ile 46
4K1L	11 beta-HSD1	457801	gamma.-Sitosterol	-9.9	Bark	Leu 217, Ala 223, Ile 46, Gly 41, Lys 44, Ile 121, Tyr 183, Val 180, Leu 126, Tyr 177
6CM4	D2 Dopamine Receptor	5286533	3-Pyrrol5-[2-(1H-benzoimidazol-2-yl)-2-cyanovinyl] furan-2-ylmorphobenzoic acid	-10.1	Bark	Asp 114, Trp 100, Val 91, Leu 94
		595533	Isoquinoline, 1-[(3,5-dibenzyloxy)benzyl]-1,2,3,4-tetrahydro-6-methoxy-	-10	Root	Leu 94, Val 91, Phe 389, Asp 114, Tyr 408
		101635021	2-Fluorenylmethyl benzoate	-9.8	Root	Val 91, Leu 94, Asp 114, Val 115, Cys 118, Phe 389, Phe 390, Thr 412
4MP2	pyruvate dehydrogenase kinase isoform 2	70385	2H-1-Benzopyran-2-one	-9.6	Root	

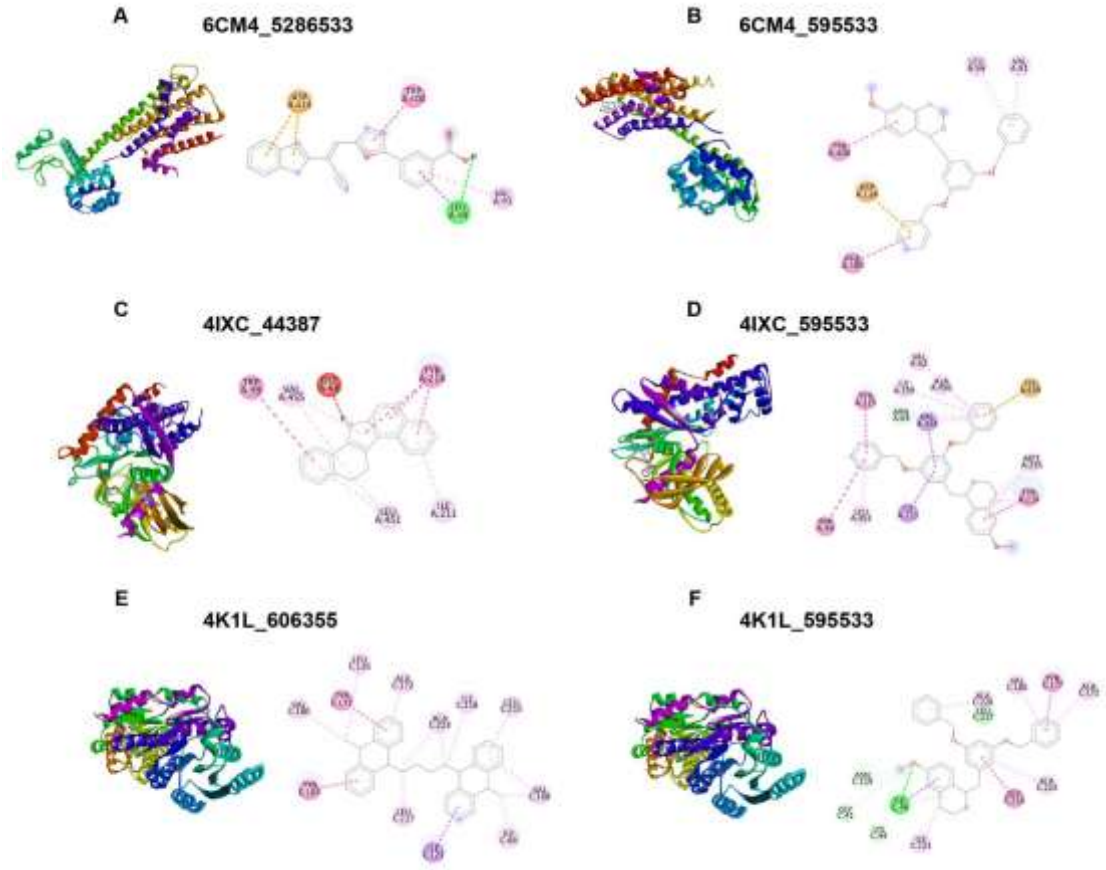

Figure 5: Docked complex of ligands with Human glucokinase (4IXC), 11-beta HSD1(4K1L) and Dopamine receptor D2 (6CM4).

A)Dopamine receptor D2 with 3-Pyrrol5-[2-(1H-benzoimidazol-2-yl)-2-cyanovinyl]furan-2-ylmorphobenzoic acid; B)Dopamine receptor D2 with Isoquinoline, 1-[(3,5-dibenzyloxy)benzyl]-1,2,3,4-tetrahydro-6-methoxy-; C) Human glucokinase with 7H-Dibenzo(a,g)carbazole, 12,13-dihydro-; D) Human glucokinase with Isoquinoline, 1-[(3,5-dibenzyloxy)benzyl]-1,2,3,4- tetrahydro-6-methoxy-; E)11-beta HSD1 with Butane, 1,4-bis(9,10-dihydro-9-methylanthracen-10-yl)-; F) 11-beta HSD1 with Isoquinoline, 1-[(3,5- dibenzyloxy)benzyl]-1,2,3,4- tetrahydro-6-methoxy-

4. Conclusion

GC-MS is one of the important techniques that provides accurate information on plant molecules of biological interest belonging to different classes of phytochemicals(Kumar et al., 2014). Virtual screening allows us to rapidly screen ligands for potential bioactivity (Gimeno et al., 2019). This study focused on screening different ligands detected in GC-MS analysis of methanolic extracts of *Crateva magna* for bioactivity against different protein targets. Our screening parameter included a cut off value of -9.6 or more with respect to the docking score to identify good drug candidates.

Docking analysis revealed that ligands identified in *C. magna* showed high affinity for only 10 specific proteins out of 57 protein targets selected for the study. Butane, 1,4-bis(9,10-dihydro-9-methylanthracen-10-yl)-(Pubchem id: 606355) a bioherbicide (Anwar et al., 2021) was shown to interact strongly with 4HOF,7CZ4,2GZ9,3FYV,4URM which are antimicrobial protein targets. Isoquinoline, 1-[(3,5- dibenzyloxy)benzyl]-1,2,3,4- tetrahydro-6-methoxy-(Pubchem id:595533) showed interactions with glucokinase (4IXC), 11β-Hydroxysteroid Dehydrogenases (4K1L), which play critical role induction of diabetes and dopamine receptor (6CM4). In addition, it also interacts with antimicrobial targets (2GZ9, 3FYV). Phenanthren-9-ylmethyl 2,6-dimethylbenzoate (Pubchem id: 605632), 7H-Dibenzo(a,g)carbazole, 12,13- dihydro- (Pubchem id:44387) and Pyrimidine-2,4,6(1H,3H,5H)-trione,5-[3-[2-(4-tertbutylphenoxy) ethoxy]benzylidene]- (Pubchem id: 633813) could be new potential drugs against diabetes as it shows affinity towards multiple diabetic targets. 3-Pyrrol5-[2-(1H-benzoimidazol-2-yl)-2-cyanovinyl] furan-2-ylmorphobenzoic acid (Pubchem id:528533) could be a potential drug against *S. aureus* as it targets both the DHFR and DNA gyrase B. Additionally, it also interacts with human 11β-Hydroxysteroid Dehydrogenases and dopamine receptors.

The inherent limitation of the study is that our screening methodology relied primarily on docking scores for the identification of potential drug targets. The future objectives include ADMET studies of the screened ligands using

SwissADME, Protox iii, and ToxTree tool. The oral bioavailibity, druglikeness and Lipinski rule screening will help understand the physico-chemical nature and drug potential of the ligands better. The lipophilicity and solubility prediction is also required to know the synthetic accessibility of the drug candidates. The docked complexes should be subjected to molecular dynamic simulation studies to understand the stability of protein backbone and the ligand interaction to protein. Pharmacophore modelling to create pharmacophore models, followed by multiple library screening can help identify the bioactive molecules that already exists which share the consonant similarity index.

FUNDING: Nil

CONFLICT OF INTEREST: All the authors declared that there is no conflict of interest to report.

5. References

1. Anwar, S., Naseem, S., Karimi, S., Asi, M. R., Akrem, A., & Ali, Z. (2021). Bioherbicidal Activity and Metabolic Profiling of Potent Allelopathic Plant Fractions Against Major Weeds of Wheat—Way Forward to Lower the Risk of Synthetic Herbicides. *Frontiers in Plant Science*, *12*, 632390. https://doi.org/10.3389/fpls.2021.632390
2. Birtwistle, J., & Baldwin, D. (1998). Role of dopamine in schizophrenia and Parkinson's disease. *British Journal of Nursing*, *7*(14), 832–841. https://doi.org/10.12968/bjon.1998.7.14.5636
3. Biovia, D.S. (2019). Discovery Studio Visualizer. San Diego.
4. Bopana, N., & Saxena, S. (2008). *Crataeva nurvala*: A Valuable Medicinal Plant. *Journal of Herbs, Spices & Medicinal Plants*, *14*(1–2), 107–127. https://doi.org/10.1080/10496470802341532
5. Bourne, C. R., Barrow, E. W., Bunce, R. A., Bourne, P. C., Berlin, K. D., & Barrow, W. W. (2010). Inhibition of Antibiotic-Resistant *Staphylococcus aureus* by the Broad-Spectrum Dihydrofolate Reductase Inhibitor RAB1. *Antimicrobial Agents and Chemotherapy*, *54*(9), 3825–3833. https://doi.org/10.1128/AAC.00361-10
6. Chapman, K., Holmes, M., & Seckl, J. (2013). 11β-Hydroxysteroid Dehydrogenases: Intracellular Gate-Keepers of Tissue Glucocorticoid Action. *Physiological Reviews*, *93*(3), 1139–1206. https://doi.org/10.1152/physrev.00020.2012
7. Chikowe, I., Bwaila, K. D., Ugbaja, S. C., & Abouzied, A. S. (2024). GC–MS analysis, molecular docking, and pharmacokinetic studies of Multidentia crassa extracts' compounds for analgesic and anti-inflammatory activities in dentistry. *Scientific Reports*, *14*(1), 1876. https://doi.org/10.1038/s41598-023-47737-x
8. Durdagi, S., Tahir Ul Qamar, M., Salmas, R. E., Tariq, Q., Anwar, F., & Ashfaq, U. A. (2018). Investigating the molecular mechanism of staphylococcal DNA gyrase inhibitors: A combined ligand-based and structure-based resources pipeline. *Journal of Molecular Graphics & Modelling*, *85*, 122–129. https://doi.org/10.1016/j.jmgm.2018.07.010
9. Fan, S., Chang, J., Zong, Y., Hu, G., & Jia, J. (2018). GC-MS Analysis of the Composition of the Essential Oil from Dendranthema indicum Var. Aromaticum Using Three Extraction Methods and Two Columns. *Molecules (Basel, Switzerland)*, *23*(3), 576. https://doi.org/10.3390/molecules23030576
10. Gimeno, A., Ojeda-Montes, M., Tomás-Hernández, S., Cereto-Massagué, A., Beltrán-Debón, R., Mulero, M., Pujadas, G., & Garcia-Vallvé, S. (2019). The Light and Dark Sides of Virtual Screening: What Is There to Know? *International Journal of Molecular Sciences*, *20*(6), 1375. https://doi.org/10.3390/ijms20061375
11. Hebbar, D. R., & Nalini, M. S. (2020). GC-MS Characterization of Antioxidative Compounds from the Stem Bark and Flower Extracts of Schefflera Species, from Western Ghats. *Der Pharmacia Lettre*, *12*(7), 51–60.
12. Jabra-Rizk, M. A., Kong, E. F., Tsui, C., Nguyen, M. H., Clancy, C. J., Fidel, P. L., & Noverr, M. (2016). Candida albicans Pathogenesis: Fitting within the Host-Microbe Damage Response Framework. *Infection and Immunity*, *84*(10), 2724–2739. https://doi.org/10.1128/IAI.00469-16
13. Jeoung, N. H. (2015). Pyruvate Dehydrogenase Kinases: Therapeutic Targets for Diabetes and Cancers. *Diabetes & Metabolism Journal*, *39*(3), 188. https://doi.org/10.4093/dmj.2015.39.3.188
14. Jeoung, N. H., Rahimi, Y., Wu, P., Lee, W. N. P., & Harris, R. A. (2012). Fasting induces ketoacidosis and hypothermia in PDHK2/PDHK4-double-knockout mice. *The Biochemical Journal*, *443*(3), 829–839. https://doi.org/10.1042/BJ20112197
15. Jin, Z., Du, X., Xu, Y., Deng, Y., Liu, M., Zhao, Y., Zhang, B., Li, X., Zhang, L., Peng, C., Duan, Y., Yu, J., Wang, L., Yang, K., Liu, F., Jiang, R., Yang, X., You, T., Liu, X., … Yang, H. (2020). Structure of Mpro from SARS-CoV-2 and discovery of its inhibitors. *Nature*, *582*(7811), 289–293. https://doi.org/10.1038/s41586-020-2223-y
16. Joy, C., & Cyriac, M. C. (2022). Phytochemicals as Potential Drug Candidates for SARS Cov-2: An RDRp Based In-Silico Drug Designing. *Proceedings of the Conference BioSangam 2022: Emerging Trends in Biotechnology (BIOSANGAM 2022)*, 58–69. https://doi.org/10.2991/978-94-6463-020-6_7
17. Juszczak, Zovko-Končić, & Tomczyk. (2019). Recent Trends in the Application of Chromatographic Techniques in the Analysis of Luteolin and Its Derivatives. *Biomolecules*, *9*(11), 731. https://doi.org/10.3390/biom9110731
18. Kumar, A., Kumari, P., & somasundaram, T. (2014). Gas Chromatography-Mass Spectrum (GC-MS) Analysis of Bioactive Components of the Methanol Extract of Halophyte, Sesuvium portulacastrum L. *International Journal of*

Advances in Pharmacy, Biology and Chemistry, *3*(3), 766–772.
19. Lee & Kim. (2019). In-Silico Molecular Binding Prediction for Human Drug Targets Using Deep Neural Multi-Task Learning. *Genes*, *10*(11), 906. https://doi.org/10.3390/genes10110906
20. Li, P., L. Snyder, G., & E. Vanover, K. (2016). Dopamine Targeting Drugs for the Treatment of Schizophrenia: Past, Present and Future. *Current Topics in Medicinal Chemistry*, *16*(29), 3385–3403. https://doi.org/10.2174/1568026616666160608084834
21. Loganayaki, N., & Manian, S. (2012). Evaluation of Indian sacred tree Crataeva magna (Lour.) DC. for antioxidant activity and inhibition of key enzymes relevant to hyperglycemia. *Journal of Bioscience and Bioengineering*, *113*(3), 378–380. https://doi.org/10.1016/j.jbiosc.2011.10.020
22. Lu, I.-L., Mahindroo, N., Liang, P.-H., Peng, Y.-H., Kuo, C.-J., Tsai, K.-C., Hsieh, H.-P., Chao, Y.-S., & Wu, S.-Y. (2006). Structure-Based Drug Design and Structural Biology Study of Novel Nonpeptide Inhibitors of Severe Acute Respiratory Syndrome Coronavirus Main Protease. *Journal of Medicinal Chemistry*, *49*(17), 5154–5161. https://doi.org/10.1021/jm060207o
23. Michelakis, E. D., Sutendra, G., Dromparis, P., Webster, L., Haromy, A., Niven, E., Maguire, C., Gammer, T.-L., Mackey, J. R., Fulton, D., Abdulkarim, B., McMurtry, M. S., & Petruk, K. C. (2010). Metabolic Modulation of Glioblastoma with Dichloroacetate. *Science Translational Medicine*, *2*(31). https://doi.org/10.1126/scitranslmed.3000677
24. Morris, G. M., Huey, R., Lindstrom, W., Sanner, M. F., Belew, R. K., Goodsell, D. S., & Olson, A. J. (2009). AutoDock4 and AutoDockTools4: Automated docking with selective receptor flexibility. *Journal of Computational Chemistry*, *30*(16), 2785–2791. https://doi.org/10.1002/jcc.21256
25. Oberacher, H., Whitley, G., & Berger, B. (2013). Evaluation of the sensitivity of the 'Wiley registry of tandem mass spectral data, MSforID' with MS/MS data of the 'NIST/NIH/EPA mass spectral library.' *Journal of Mass Spectrometry*, *48*(4), 487–496. https://doi.org/10.1002/jms.3184
26. Paulsen, J. L., Bendel, S. D., & Anderson, A. C. (2011). Crystal Structures of *Candida albicans* Dihydrofolate Reductase Bound to Propargyl-Linked Antifolates Reveal the Flexibility of Active Site Loop Residues Critical for Ligand Potency and Selectivity. *Chemical Biology & Drug Design*, *78*(4), 505–512. https://doi.org/10.1111/j.1747-0285.2011.01169.x
27. Peng, K., Pan, Y., Li, J., Khan, Z., Fan, M., Yin, H., Tong, C., Zhao, Y., Liang, G., & Zheng, C. (2016). 11β-Hydroxysteroid Dehydrogenase Type 1(11β-HSD1) mediates insulin resistance through JNK activation in adipocytes. *Scientific Reports*, *6*(1), 37160. https://doi.org/10.1038/srep37160
28. Poongattil,S., Thomas, J. & Cheruthazhakkat, S. High-performance thin-layer chromatography profiling of Crateva magna (Lour.) DC. from different parts of South India. (2024). *JPC-J Planar Chromat* . https://doi.org/10.1007/s00764-024-00294-z
29. Prabhat, D., Ranjan, S., Mekap.S, & Pani, S. (2010). Phytochemical and Pharmacological Screening of the Plant Crateva Magna Against Alloxan Induced Diabetes in Rats. *Journal of Pharmaceutical Sciences and Research*, *2*.
30. Premila, M. (1995). *Premila MS, Ayurvedic Herbs: A Clinical Guide to the Healing Plants of Traditional Indian Medicine, In: Plants for urinary tract disorders, 5th Edn, 1995, pp. 157-160.* (5th ed.).
31. Ren, Y., Li, L., Wan, L., Huang, Y., & Cao, S. (2022). Glucokinase as an emerging anti-diabetes target and recent progress in the development of its agonists. *Journal of Enzyme Inhibition and Medicinal Chemistry*, *37*(1), 606–615. https://doi.org/10.1080/14756366.2021.2025362
32. Russell, C. W., Richards, A. C., Chang, A. S., & Mulvey, M. A. (2017). The Rhomboid Protease GlpG Promotes the Persistence of Extraintestinal Pathogenic Escherichia coli within the Gut. *Infection and Immunity*, *85*(6), e00866-16. https://doi.org/10.1128/IAI.00866-16
33. Samdani, A., & Vetrivel, U. (2018). POAP: A GNU parallel based multithreaded pipeline of open babel and AutoDock suite for boosted high throughput virtual screening. *Computational Biology and Chemistry*, *74*, 39–48. https://doi.org/10.1016/j.compbiolchem.2018.02.012
34. Sameen, S., Khalid, Z., & Malik, S. I. (2013). Role of pyruvate dehydrogenase kinases (PDK's) and their respective microRNA's in human ovarian cancer. *Global Journal of Molecular Evolution and Genomics*, *1*(1), 56–62.
35. Sethi, V., Jain, M., & Thakur, R. (1978). Chemical constituents of Crataeva religiosa. *Plant Med*, *34*, 223–224.
36. Shaker, B., Ahmad, S., Lee, J., Jung, C., & Na, D. (2021). In silico methods and tools for drug discovery. *Computers in Biology and Medicine*, *137*, 104851. https://doi.org/10.1016/j.compbiomed.2021.104851
37. Sharma, P., Singh, S., Sharma, N., Singla, D., Guarve, K., & Grewal, A. S. (2022). Targeting human Glucokinase for the treatment of type 2 diabetes: An overview of allosteric Glucokinase activators. *Journal of Diabetes & Metabolic Disorders*, *21*(1), 1129–1137. https://doi.org/10.1007/s40200-022-01019-x
38. Singh, G., Soni, H., Tandon, S., Kumar, V., Babu, G., Gupta, V., & Chaudhuri (Chattopadhyay), P. (2022). Identification of natural DHFR inhibitors in MRSA strains: Structure-based drug design study. *Results in Chemistry*, *4*, 100292. https://doi.org/10.1016/j.rechem.2022.100292
39. Staniszewska, M., Bondaryk, M., Piłat, J., Siennicka, K., Magda, U., & Kurzatkowski, W. (2012). [Virulence factors of Candida albicans]. *Przeglad Epidemiologiczny*, *66*(4), 629–633.
40. Sun, H., Zhu, A., Zhou, X., & Wang, F. (2017). Suppression of pyruvate dehydrogenase kinase-2 re-sensitizes

paclitaxel-resistant human lung cancer cells to paclitaxel. *Oncotarget*, *8*(32), 52642–52650. https://doi.org/10.18632/oncotarget.16991

41. Trott, O., & Olson, A. J. (2009). AutoDock Vina: Improving the speed and accuracy of docking with a new scoring function, efficient optimization, and multithreading. *Journal of Computational Chemistry*, NA-NA. https://doi.org/10.1002/jcc.21334
42. Vidal-Limon, A., Aguilar-Toalá, J. E., & Liceaga, A. M. (2022). Integration of Molecular Docking Analysis and Molecular Dynamics Simulations for Studying Food Proteins and Bioactive Peptides. *Journal of Agricultural and Food Chemistry*, *70*(4), 934–943. https://doi.org/10.1021/acs.jafc.1c06110
43. Vijayakumari, B., Sasikala, V., Radha, S. R., & Rameshwar, H. Y. (2016). In silico analysis of aqueous root extract of Rotula aquatica Lour for docking analysis of the compound 3-O-acetyl-11-keto-β-boswellic acid contents. *SpringerPlus*, *5*(1), 1486. https://doi.org/10.1186/s40064-016-3134-0
44. Wang, X., Shen, X., Yan, Y., & Li, H. (2021). Pyruvate dehydrogenase kinases (PDKs): An overview toward clinical applications. *Bioscience Reports*, *41*(4), BSR20204402. https://doi.org/10.1042/BSR20204402
45. Weinberg, R. A., McWherter, C. A., Freeman, S. K., Wood, D. C., Gordon, J. I., & Lee, S. C. (1995). Genetic studies reveal that myristoylCoA:protein N-myristoyltransferase is an essential enzyme in *Candida albicans*. *Molecular Microbiology*, *16*(2), 241–250. https://doi.org/10.1111/j.1365-2958.1995.tb02296.x